

# Adaptive Super-twisting Integral Terminal Sliding Mode Control Design for Quadrotors

Qianyu Feng

**Abstract**— In this study, a novel adaptive hyper-spiral integral terminal sliding mode control (ASTITSMC) algorithm was designed. No prior knowledge of the boundary and gradient of the disturbance was required. The dynamic gain ensured robustness against external disturbances, reduced the chattering of the control input, and effectively suppressed the chattering. The designed sliding surface combines the non-singular terminal sliding mode and integral sliding mode, solving the singularity problem existing in traditional terminal sliding mode control and achieving global non-singular control of the system. By introducing an integral term on the sliding surface, all moments of the sliding control are in a stable state, not only ensuring the global asymptotic stability of the system, but also effectively avoiding the chattering phenomenon caused by high-frequency switching control. Finally, simulation experiments and result analysis were conducted for the adaptive hyper-spiral using integral terminal sliding mode (ASTLSMC) and terminal sliding mode (ASTTSMC). ASTITSMC has smaller steady-state error, faster response speed, and more accurate trajectory tracking ability compared to ASTLSMC and ASTTSMC algorithms, and performs better in reducing the chattering phenomenon in the control process.

**Index Terms**—Adaptive control, Super-twisting algorithm, integral terminal sliding mode control, Quadrotor

## I. INTRODUCTION

In recent years, due to the advantages of vertical take-off and landing, high-speed maneuverability, hovering capability, high performance, small size and low cost, quadrotors have been widely used in reconnaissance [1], mapping [2], surveillance [3], rescue [4], search [5] and other military and civilian applications. However, it is difficult to achieve accurate control of the quadrotor due to the highly coupled nonlinear dynamics, underactuated, parameter uncertainties, and external disturbances.

Currently, numerous control strategies have been proposed for quadrotor position and attitude control, such as robust control [6], optimal control [7], adaptive control [8], intelligent control [9], and sliding mode control (SMC) [10]. Despite the successful development and implementation of several nonlinear controllers, the design of robust and efficient flight controllers remains a research focus. Sliding mode control achieves rapid and precise control of the system by designing a sliding surface (or switching surface), allowing the system's state to move on this sliding surface. Due to the advantages of sliding mode control, such as fast response speed, excellent transient performance, ease of implementation, and robustness against external disturbances

and model uncertainties, it is often used in the design of controllers for the position and attitude tracking of quadrotor unmanned aerial vehicles.

Reference [11] proposed a four-rotor position and attitude tracking control strategy based on second-order linear sliding mode (LSMC). Although this strategy achieved trajectory tracking, the linear sliding mode could not guarantee the finite-time convergence of the system. To address this issue, in [12], terminal sliding mode (TSMC) was introduced to accelerate the convergence speed and ensure the finite-time system convergence. To obtain a fast transient convergence rate in the range far from and close to the equilibrium point, in [13], a fast terminal sliding mode (FTSMC) was proposed. This control strategy combines the advantages of terminal sliding mode and linear sliding mode, providing control performance that cannot be achieved by using these methods alone. With the research on sliding mode control, it was found that both the terminal sliding mode method and the fast terminal sliding mode method may have singularity phenomena. To solve the singularity problem, reference [14] proposed non-singular terminal sliding mode control (NTSMC), which solved the singularity problem of the traditional terminal sliding mode by introducing nonlinear terms. Reference [15] proposed a new sliding mode control strategy, the non-singular fast terminal sliding mode (NFTSMC), based on the non-singular terminal sliding mode and the fast terminal sliding mode control strategy, achieving fast convergence and high-precision tracking of the system. Reference [16] proposed an integral terminal sliding mode (ITSMC) control method to solve the singularity problem of systems with multiple inputs and multiple outputs in relative first-order systems.

Although the traditional sliding mode control strategy has the advantages of robustness, rapid response and precise tracking, it also has some drawbacks, such as high-frequency jitter phenomenon and insufficient control accuracy. To solve the problem of high-frequency jitter, researchers have proposed various improvement methods, such as adaptive sliding mode control and super-spiral sliding mode control methods. For the finite-time position and attitude tracking problem of a quadcopter with input delay, model uncertainty and external disturbances, reference [17] proposed a terminal sliding mode control method based on an adaptive strategy. Under the assumption of bounded but unknown model uncertainty and external disturbances, the adaptive strategy is used to estimate the upper bound, ensuring the global finite-time stability of the system. In reference [18], a controller based on backstepping and non-singular terminal sliding mode was designed, combined with the adaptive strategy to achieve trajectory tracking control of the quadcopter. Super-spiral (STA) is an effective tool to

Manuscript received May 15, 2025

Qianyu Feng, School of Computer Science and Technology, Tiangong University, Tianjin, 300387, China

suppress jitter and has gradually become a research hotspot. The main disadvantage of STA is that it requires knowing the upper bound of the disturbance gradient, which is often challenging in practical scenarios. Overestimating this boundary will lead to unnecessary high control gains, which will reduce the system performance.

In this study, combines two chattering suppression methods: gain adaptive and super-spiral sliding mode control, and proposes an adaptive super-spiral integral terminal sliding mode control (ASTISMC) algorithm with time-varying disturbances. The proposed control scheme combines the equivalent control law and the adaptive super-spiral control law, further improving the convergence speed and tracking accuracy of the system. By introducing the integral term on the sliding surface, all moments of the sliding mode control can be in a stable state. The main contributions of this article are as follows:

- Considering the dynamical equations of a quadrotor system with six degrees of freedom subjected to uncertain bounded disturbances.
- An ASTISMC is proposed for attitude control of quadrotor with time-varying disturbances. By adaptively dynamically adjusting the control gain to reduce chattering while maintaining robustness to uncertainties and disturbances.
- The designed sliding surface combines the non-singular terminal sliding mode and integral sliding mode, avoiding the singularity problem existing in traditional terminal sliding mode control, while improving the convergence accuracy while ensuring the fast response speed.

The rest of the paper is structured as follows: Section 2 describes the dynamic model of the quadrotor and some Preparations. An ASTISMC controller is designed for the position and attitude subsystems of the quadrotor. A finite-time stability proof is presented in Section 3. A set of comparisons with ASTLSMC, ASTTSMC controllers is presented in Section 4. Section 5 presents some conclusions of this paper and future work.

## II. PREPARATIO AND PROBLEM DESCRIPTION

This chapter focuses on the position and attitude trajectory tracking control of quadrotor unmanned aerial vehicles. Firstly, the following assumptions are proposed:

Assumption 1: The expected trajectory is continuous and twice differentiable.

Assumption 2: The disturbance is unknown but bounded.

$$|\dot{d}_i| \leq \xi_i, \xi_i > 0 (i = x, y, z, \phi, \theta, \psi).$$

Assumption 3: Roll angle and pitch angle are both in the region  $(-\frac{\pi}{2}, \frac{\pi}{2})$ .

The coupling characteristics of the quadrotor unmanned aerial vehicle mainly manifest in the coupling between position control and attitude control, as well as the coupling among different attitude degrees of freedom. The only four independent control inputs of the quadrotor unmanned aerial vehicle cannot directly achieve the tracking control of six degrees of freedom. To achieve real-time tracking of the position and attitude of the quadrotor unmanned aerial vehicle, an effective control strategy is to track the position and yaw angle, while ensuring the stability of the other two

attitudes. For this purpose, a cascaded control strategy can be adopted. Firstly, a virtual controller for the position loop is set up to ensure the precise tracking of the position loop channel, and the required attitude angles  $\phi_d$  and  $\theta_d$  are generated by the actual control quantity and transmitted  $u_1$  to the attitude control subsystem.

Consider the dynamics equation of the quadrotor as follows:

$$\begin{cases} \dot{x}_1 = x_2 \\ \dot{x}_2 = \frac{1}{m}(\cos x_7 \sin x_9 \cos x_{11} + \sin x_7 \sin x_{11})U_1 - c_1 x_2 + d_x \\ \dot{x}_3 = x_4 \\ \dot{x}_4 = \frac{1}{m}(\cos x_7 \sin x_9 \sin x_{11} - \sin x_7 \cos x_{11})U_1 - c_2 x_4 + d_y \\ \dot{x}_5 = x_6 \\ \dot{x}_6 = \frac{1}{m}(\cos x_7 \cos x_9)U_1 - g - c_3 x_6 + d_z \\ \dot{x}_7 = x_8 \\ \dot{x}_8 = a_1 x_{10} x_{12} + b_1 \Omega_r x_{10} + f_1 U_2 - c_4 x_8 + d_\phi \\ \dot{x}_9 = x_{10} \\ \dot{x}_{10} = a_2 x_8 x_{12} - b_2 \Omega_r x_8 + f_2 U_3 - c_5 x_{10} + d_\theta \\ \dot{x}_{11} = x_{12} \\ \dot{x}_{12} = a_3 x_8 x_{10} + f_3 U_4 - c_6 x_{12} + d_\psi \end{cases} \quad (1)$$

where  $a_1 = (J_y - J_z)/J_x$ ,  $a_2 = (J_z - J_x)/J_y$ ,

$$a_3 = (J_x - J_y)/J_z, b_1 = J_r/J_y, c_1 = K_x/m,$$

$$c_2 = K_y/m, c_3 = K_z/m, c_4 = K_\phi/J_x,$$

$$c_5 = K_\theta/J_y, c_6 = K_\psi/J_z, f_1 = 1/J_x, f_2 = 1/J_x,$$

$$f_3 = 1/J_y, f_4 = 1/J_z.$$

The Virtual control input  $[u_x, u_y, u_z]^T$  can be expressed as:

$$\begin{cases} u_x = (\sin \phi \sin \psi + \cos \phi \sin \theta \cos \psi)U_1 \\ u_y = (-\sin \phi \cos \psi + \cos \phi \sin \theta \sin \psi)U_1 \\ u_z = (\cos \theta \cos \phi)U_1 \end{cases} \quad (2)$$

According to the above formula, the following  $u_1$  and  $(\phi_d, \theta_d)$  can be calculated:

$$\begin{cases} \phi_d = \arcsin\left(\frac{u_x \sin \psi_d - u_y \cos \psi_d}{u_1}\right) \\ \theta_d = \arctan\left(\frac{u_x \cos \psi_d + u_y \sin \psi_d}{u_z}\right) \\ U_1 = [u_x^2 + u_y^2 + u_z^2]^{\frac{1}{2}} \end{cases} \quad (3)$$

## III. CONTROLLER DESIGN AND STABILITY ANALYSIS

The position controller and attitude controller for the quadrotor unmanned aerial vehicle will be designed in detail. To enhance the trajectory tracking performance of the system, the proposed control scheme will combine the equivalent control law and the adaptive super-spiral control law.

### A. Equivalent Control Law Design

Define the tracking error of the position subsystem of the quadcopter unmanned aerial vehicle:

$$\begin{cases} e_1 = e_x = x_1 - x_{1d} \\ e_2 = e_y = x_3 - x_{3d} \\ e_3 = e_z = x_5 - x_{5d} \end{cases} \quad (4)$$

Using integral terminal sliding mode control enables the system to be on the sliding surface from the very beginning, eliminating the process of the system state reaching the sliding surface from the initial position. This accelerates the convergence of the system. Based on this, the following non-singular integral terminal sliding surface is defined:

$$S_\delta = \dot{e}_\delta + \int [\lambda_{1\delta} sig(e_\delta)^{\gamma_{1\delta}} + \lambda_{2\delta} sig(\dot{e}_\delta)^{\gamma_{2\delta}}] \quad (5)$$

where  $\gamma_{1p}, \gamma_{2p}$  is a positive control parameter.  $sig(x)^\delta$  is a monotonically increasing smooth function that can be expressed as:

$$sig(x)^\delta = |x|^\delta sgn(x) \quad (6)$$

Let  $\dot{S}_\delta = 0$ , the equivalent control law for the position subsystem can be obtained as follows:

$$\begin{cases} U_{eqx} = m[c_1 x_2 + \ddot{x}_{1d} - \lambda_{1x} |e_x|^{\gamma_{1x}} sig(e_x) - \lambda_{2x} |\dot{e}_x|^{\gamma_{2x}} sig(\dot{e}_x)] \\ U_{eqy} = m[c_2 x_4 + \ddot{x}_{3d} - \lambda_{1y} |e_y|^{\gamma_{1y}} sig(e_y) - \lambda_{2y} |\dot{e}_y|^{\gamma_{2y}} sig(\dot{e}_y)] \\ U_{eqz} = m[c_3 x_6 + \ddot{x}_{5d} + g - \lambda_{1z} |e_z|^{\gamma_{1z}} sig(e_z) - \lambda_{2z} |\dot{e}_z|^{\gamma_{2z}} sig(\dot{e}_z)] \end{cases} \quad (7)$$

Define the tracking error of the attitude subsystem of a quadcopter unmanned aerial vehicle:

$$\begin{cases} e_4 = e_\phi = x_7 - x_{7d} \\ e_5 = e_\theta = x_9 - x_{9d} \\ e_6 = e_\psi = x_{11} - x_{11d} \end{cases} \quad (8)$$

The non-singular integral terminal sliding surface of the attitude subsystem is defined as:

$$S_\ominus = \dot{e}_\ominus + \int [\lambda_{1\ominus} |e_\ominus|^{\gamma_{1\ominus}} sig(e_\ominus) + \lambda_{2\ominus} |\dot{e}_\ominus|^{\gamma_{2\ominus}} sig(\dot{e}_\ominus)] \quad (9)$$

The equivalent control law of the attitude subsystem is:

$$\begin{cases} U_{eq\phi} = f_1^{-1}[c_4 x_8 + \ddot{x}_{7d} - a_1 x_{10} x_{12} - b_1 \Omega_r x_{10} - \lambda_{1\phi} |e_\phi|^{\gamma_{1\phi}} sig(e_\phi) - \lambda_{2\phi} |\dot{e}_\phi|^{\gamma_{2\phi}} sig(\dot{e}_\phi)] \\ U_{eq\theta} = f_2^{-1}[c_5 x_{10} + \ddot{x}_{9d} - a_2 x_8 x_{12} + b_2 \Omega_r x_8 - \lambda_{1\theta} |e_\theta|^{\gamma_{1\theta}} sig(e_\theta) - \lambda_{2\theta} |\dot{e}_\theta|^{\gamma_{2\theta}} sig(\dot{e}_\theta)] \\ U_{eq\psi} = f_3^{-1}[c_6 x_{12} + \ddot{x}_{11d} - a_3 x_8 x_{10} - \lambda_{1\psi} |e_\psi|^{\gamma_{1\psi}} sig(e_\psi) - \lambda_{2\psi} |\dot{e}_\psi|^{\gamma_{2\psi}} sig(\dot{e}_\psi)] \end{cases} \quad (10)$$

### B. Adaptive Superhelix Control Law Design

In this chapter, an adaptive hyper-spiral control law is adopted to construct the switching strategy, and it is combined with the equivalent control strategy designed in the previous part to achieve precise tracking control of the position and attitude of the quadrotor unmanned aerial vehicle.

The adaptive hyper-spiral control law of the position subsystem is:

$$\begin{cases} U_{swx} = m[-\zeta_{1x} |S_x|^{\frac{1}{2}} sig(S_x) - \int \zeta_{2x} sig(S_x) dt] \\ U_{swy} = m[-\zeta_{1y} |S_y|^{\frac{1}{2}} sig(S_y) - \int \zeta_{2y} sig(S_y) dt] \\ U_{swz} = m[-\zeta_{1z} |S_z|^{\frac{1}{2}} sig(S_z) - \int \zeta_{2z} sig(S_z) dt] \end{cases} \quad (11)$$

The adaptive hyper-spiral control law of the attitude subsystem is:

$$\begin{cases} U_{sw\phi} = f_1^{-1}[-\zeta_{1\phi} |S_\phi|^{\frac{1}{2}} sig(S_\phi) - \int \zeta_{2\phi} sig(S_\phi) dt] \\ U_{sw\theta} = f_2^{-1}[-\zeta_{1\theta} |S_\theta|^{\frac{1}{2}} sig(S_\theta) - \int \zeta_{2\theta} sig(S_\theta) dt] \\ U_{sw\psi} = f_3^{-1}[-\zeta_{1\psi} |S_\psi|^{\frac{1}{2}} sig(S_\psi) - \int \zeta_{2\psi} sig(S_\psi) dt] \end{cases} \quad (12)$$

where  $S_\ominus = [S_\phi, S_\theta, S_\psi]^T$ ,  $\zeta_{1\ominus} = [\zeta_{1\phi}, \zeta_{1\theta}, \zeta_{1\psi}]^T$ ,

$\zeta_{2\ominus} = [\zeta_{2\phi}, \zeta_{2\theta}, \zeta_{2\psi}]^T$ .  $\zeta_{1\delta}, \zeta_{2\delta}, \zeta_{1\ominus}, \zeta_{2\ominus}$  is the adaptive control gain to be designed.

The main drawback of the super-helix controller is that it requires knowledge of the upper bound of external disturbances, which is often difficult to achieve in many practical situations. Overestimating the boundary of the disturbance will lead to unnecessary high control gains, causing the system to shake and become unstable. This will reduce the system performance. Moreover, high gains may also cause the controller output to saturate, limiting the ability to reduce errors or disturbances. To prevent overestimation of the control gain, an adaptive gain  $\zeta_{1\delta}, \zeta_{2\delta}, \zeta_{1\ominus}, \zeta_{2\ominus}$  will be incorporated into the super-helix.

The expression  $\zeta_{1\delta}, \zeta_{2\delta}, \zeta_{1\ominus}, \zeta_{2\ominus}$  is as follows:

$$\zeta_{1\delta} = \begin{cases} \varepsilon_\delta \left(\frac{g_\delta}{2}\right)^{\frac{1}{2}} sig(|S_\delta| - \mu_\delta) & \zeta_{1\delta} > \zeta_{m\delta} \\ \eta_\delta & \zeta_{1\delta} \leq \zeta_{m\delta} \end{cases} \quad (13)$$

$$\zeta_{2\delta} = 2\tau_\delta \zeta_{1\delta}$$

$$\zeta_{1\ominus} = \begin{cases} \varepsilon_\ominus \left(\frac{g_\ominus}{2}\right)^{\frac{1}{2}} sig(|S_\ominus| - \mu_\ominus) & \zeta_{1\ominus} > \zeta_{m\ominus} \\ \eta_\ominus & \zeta_{1\ominus} \leq \zeta_{m\ominus} \end{cases} \quad (14)$$

$$\zeta_{2\ominus} = 2\tau_\ominus \zeta_{1\ominus}$$

Based on the equivalent control laws of the position subsystem and the attitude subsystem designed in the previous text, the trajectory tracking control laws for the position subsystem and the attitude subsystem of the quadrotor unmanned aerial vehicle can be obtained as follows:

$$u = u_{eq} + u_{sw} \quad (15)$$

where  $u = [u_x, u_y, u_z, u_\phi, u_\theta, u_\psi]^T$

$$u_{eq} = [u_{eqx}, u_{eqy}, u_{eqz}, u_{eq\phi}, u_{eq\theta}, u_{eq\psi}]^T,$$

$$u_{sw} = [u_{swx}, u_{swy}, u_{swz}, u_{sw\phi}, u_{sw\theta}, u_{sw\psi}]^T$$

### C. Proof

This section aims to conduct a stability analysis of the position and attitude tracking control algorithm for the

quadrotor unmanned aerial vehicle, in order to confirm that the control strategy proposed in the previous text can ensure that the system state reaches the designed sliding surface within a limited time. The stability proofs for the position subsystem and attitude subsystem controllers are the same. Below, we will take the stability proof of the position subsystem as an example.

First, the system is analyzed, and a new state vector is introduced to facilitate Lyapunov analysis. Its expression is as follows:

$$Z_\delta = [z_{1\delta}, z_{2\delta}]^T = [|S_\delta|^{\frac{1}{2}} \text{sign}(S_\delta) \quad \Gamma_\delta]^T \quad (15)$$

Taking the derivative in (15) yields:

$$\begin{cases} \dot{z}_{1\delta} = \frac{1}{2|z_{1\delta}|}(-\zeta_{1\delta}|S_\delta|^{\frac{1}{2}} \text{sign}(S_\delta) + \Gamma_\delta) \\ \quad = \frac{1}{2|z_{1\delta}|}(-\zeta_{1\delta}z_{1\delta} + z_{2\delta}) \\ \dot{z}_{2\delta} = -\zeta_{2\delta} \text{sign}(S_\delta) |S_\delta|^{\frac{1}{2}} |S_\delta|^{\frac{1}{2}} \\ \quad = \frac{1}{2|z_{1\delta}|}(-2\zeta_{2\delta}z_{1\delta}) \end{cases} \quad (16)$$

In the above equation,  $\frac{1}{|z_{1\delta}|} = |S_\delta|^{\frac{1}{2}}$

$V_0(Z_\delta)$  and the Lyapunov function  $V(Z_\delta, \zeta_{1\delta}, \zeta_{2\delta})$  is defined as  $(4\tau_\delta)z_{1\delta}z_{2\delta}$  (17)

where  $P_\delta = \begin{bmatrix} \xi_\delta + 4\tau_\delta^2 & -2\tau_\delta \\ -2\tau_\delta & 1 \end{bmatrix}$ .

It can be concluded that all the eigenvalues of the matrix are greater than 0, making it a positive definite matrix. Taking the derivatives of the Lyapunov function equation from both sides gives:

$$\begin{aligned} \dot{V}_0(Z_\delta) &= \dot{Z}_\delta^T P_\delta Z_\delta + Z_\delta^T P_\delta \dot{Z}_\delta \\ &= (N_\delta Z_\delta)^T P_\delta Z_\delta + Z_\delta^T P_\delta (N_\delta Z_\delta) \\ &= -\frac{1}{2|z_{1\delta}|} Z_\delta^T Q_\delta Z_\delta \end{aligned} \quad (18)$$

The expression of the matrix  $Q_\delta$  is as follows:

$$Q_\delta = \begin{bmatrix} 2\zeta_{1\delta}(\xi_\delta + 4\tau_\delta^2) - 8\zeta_{2\delta}\tau_\delta & -\xi_\delta - 4\tau_\delta^2 - 2\zeta_{1\delta}\tau_\delta + 2\zeta_{2\delta} \\ -\xi_\delta - 4\tau_\delta^2 - 2\zeta_{1\delta}\tau_\delta + 2\zeta_{2\delta} & 4\tau_\delta \end{bmatrix}$$

In order to ensure the positive definiteness of the matrix  $Q_\delta$ . Let  $\lambda_{\min}(Q_\delta) > 2\tau > 0$ , is required to be satisfied

$$\zeta_{1\delta} > \frac{4\tau_\delta^2 + (\xi_\delta + 4\tau_\delta^2)^2}{8\tau_\delta \xi_\delta}$$

By  $\lambda_{\min}(Q_\delta) \|Z_\delta\|^2 \leq Z_\delta^T Q_\delta Z_\delta \leq \lambda_{\max}(Q_\delta) \|Z_\delta\|^2$ , can be obtained:

$$\dot{V}_{(0)}(Z_\delta) \leq -\frac{2\tau_\delta}{2|z_{1\delta}|} Z_\delta^T Z_\delta = -\frac{\tau_\delta}{|z_{1\delta}|} \|Z_\delta\|^2 \quad (19)$$

By  $|z_{1\delta}| = |S_\delta|^{\frac{1}{2}} \leq \|Z_\delta\| \leq \frac{V_{(0)}^{\frac{1}{2}}(Z_\delta)}{\lambda_{\min}^{\frac{1}{2}}(P_\delta)}$

$$\dot{V}_{(0)}(Z_\delta) \leq -\frac{\tau_\delta \lambda_{\min}^{\frac{1}{2}}(P_\delta)}{\lambda_{\max}^{\frac{1}{2}}(P_\delta)} V_{(0)}^{\frac{1}{2}}(Z_\delta) \quad (20)$$

We can obtain  $\dot{V}_0(Z_\delta) \leq -\ell_\delta V_0^{\frac{1}{2}}$ , among them

$$\ell_\delta = -\tau_\delta \lambda_{\min}^{\frac{1}{2}}(P_\delta) / \lambda_{\max}^{\frac{1}{2}}(P_\delta).$$

Under the adaptive law, the maximum value of  $\zeta_{1\delta}$ ,  $\zeta_{2\delta}$  is  $\bar{\zeta}_{1\delta}$ ,  $\bar{\zeta}_{2\delta}$ . It can be concluded that:

$$\bar{\zeta}_{1\delta} = \zeta_{1\delta} - \zeta_{1\delta}^* < 0, \quad \bar{\zeta}_{2\delta} = \zeta_{2\delta} - \zeta_{2\delta}^* < 0 \quad (21)$$

Consider the following Lyapunov function:

$$\begin{aligned} V(Z_\delta, \zeta_{1\delta}, \zeta_{2\delta}) &= V_0(Z_\delta) + \frac{1}{2\mathcal{G}_{1\delta}} (\zeta_{1\delta} - \zeta_{1\delta}^*)^2 \\ &\quad + \frac{1}{2\mathcal{G}_{2\delta}} (\zeta_{2\delta} - \zeta_{2\delta}^*)^2 \end{aligned} \quad (22)$$

$$\begin{aligned} \dot{V}(Z_\delta, \zeta_{1\delta}, \zeta_{2\delta}) &\leq -\ell V_0^{\frac{1}{2}} - \frac{\varepsilon_{1\delta}}{\sqrt{2\mathcal{G}_{1\delta}}} |\bar{\zeta}_{1\delta}| - \frac{\varepsilon_{2\delta}}{\sqrt{2\mathcal{G}_{2\delta}}} |\bar{\zeta}_{2\delta}| \\ &\quad + \frac{\bar{\zeta}_{1\delta} \dot{\zeta}_{1\delta}}{\mathcal{G}_{1\delta}} + \frac{\bar{\zeta}_{2\delta} \dot{\zeta}_{2\delta}}{\mathcal{G}_{2\delta}} + \frac{\varepsilon_{1\delta}}{\sqrt{2\mathcal{G}_{1\delta}}} |\bar{\zeta}_{1\delta}| + \frac{\varepsilon_{2\delta}}{\sqrt{2\mathcal{G}_{2\delta}}} |\bar{\zeta}_{2\delta}| \\ &\leq -\sqrt{\ell^2 V_0 + \frac{\varepsilon_{1\delta}^2}{2\mathcal{G}_{1\delta}} |\bar{\zeta}_{1\delta}|^2 + \frac{\varepsilon_{2\delta}^2}{2\mathcal{G}_{2\delta}} |\bar{\zeta}_{2\delta}|^2} + \frac{\bar{\zeta}_{1\delta} \dot{\zeta}_{1\delta}}{\mathcal{G}_{1\delta}} \\ &\quad + \frac{\bar{\zeta}_{2\delta} \dot{\zeta}_{2\delta}}{\mathcal{G}_{2\delta}} + \frac{\varepsilon_{1\delta}}{\sqrt{2\mathcal{G}_{1\delta}}} |\bar{\zeta}_{1\delta}| + \frac{\varepsilon_{2\delta}}{\sqrt{2\mathcal{G}_{2\delta}}} |\bar{\zeta}_{2\delta}| \\ &\leq -\alpha_0 [V(Z_\delta, \zeta_{1\delta}, \zeta_{2\delta})]^{1/2} - |\bar{\zeta}_{1\delta}| \left( \frac{\dot{\zeta}_{1\delta}}{\mathcal{G}_{1\delta}} - \frac{\varepsilon_{1\delta}}{\sqrt{2\mathcal{G}_{1\delta}}} \right) \\ &\quad - |\bar{\zeta}_{2\delta}| \left( \frac{\dot{\zeta}_{2\delta}}{\mathcal{G}_{2\delta}} - \frac{\varepsilon_{2\delta}}{\sqrt{2\mathcal{G}_{2\delta}}} \right) \end{aligned} \quad (23)$$

In the above equation:  $\alpha_0 = \min(\ell_\delta, \varepsilon_{1\delta}, \varepsilon_{2\delta})$ . Let

$\chi_\delta = |\bar{\zeta}_{1\delta}| \left( \frac{\dot{\zeta}_{1\delta}}{\mathcal{G}_{1\delta}} - \frac{\varepsilon_{1\delta}}{\sqrt{2\mathcal{G}_{1\delta}}} \right) + |\bar{\zeta}_{2\delta}| \left( \frac{\dot{\zeta}_{2\delta}}{\mathcal{G}_{2\delta}} - \frac{\varepsilon_{2\delta}}{\sqrt{2\mathcal{G}_{2\delta}}} \right)$  Regarding  $t \geq 0$ , Suppose  $|S_\delta| > \mu_\delta$ ,  $\zeta_{1\delta} > \zeta_{m\delta}$ , Therefore, it can be concluded that:  $\frac{\dot{\zeta}_{1\delta}}{\mathcal{G}_{1\delta}} - \frac{\varepsilon_{1\delta}}{\sqrt{2\mathcal{G}_{1\delta}}} = 0$ . Therefore

$$\chi_\delta = |\bar{\zeta}_{2\delta}| \left( \frac{\dot{\zeta}_{2\delta}}{\mathcal{G}_{2\delta}} - \frac{\varepsilon_{2\delta}}{\sqrt{2\mathcal{G}_{2\delta}}} \right) \quad (24)$$

Let  $\tau_\delta = \varepsilon_{2\delta} / 2\varepsilon_{1\delta} \sqrt{\mathcal{G}_{2\delta} / \mathcal{G}_{1\delta}}$ , it can be concluded that:

$$\begin{aligned} \chi_\delta &= |\bar{\zeta}_{2\delta}| \left( \frac{\varepsilon_{2\delta}}{\varepsilon_{1\delta}} \sqrt{\frac{\mathcal{G}_{2\delta}}{\mathcal{G}_{1\delta}}} \dot{\zeta}_{1\delta} - \frac{\varepsilon_{2\delta}}{\sqrt{2\mathcal{G}_{2\delta}}} \right) \\ &= |\bar{\zeta}_{2\delta}| \left( \frac{\varepsilon_{2\delta}}{\varepsilon_{1\delta}} \sqrt{\frac{\mathcal{G}_{2\delta}}{\mathcal{G}_{1\delta}}} \varepsilon_{1\delta} \left( \frac{\mathcal{G}_{1\delta}}{2} \right)^{\frac{1}{2}} - \frac{\varepsilon_{2\delta}}{\sqrt{2\mathcal{G}_{2\delta}}} \right) = 0 \end{aligned} \quad (25)$$

$$\dot{V}(Z_\delta, \zeta_{1\delta}, \zeta_{2\delta}) \leq -\alpha_0 [V(Z_\delta, \zeta_{1\delta}, \zeta_{2\delta})]^{1/2} \quad (26)$$

According to the theory of finite-time stability, the state of

the position subsystem of the quadcopter will reach a stable state within a finite period of time.

$$T(x_0) \leq \frac{2}{\alpha_0} V^{\frac{1}{2}}(Z_\delta, \zeta_{1\delta}, \zeta_{2\delta}) \quad (27)$$

#### IV. SIMULATION RESULTS AND EXPERIMENTAL ANALYSIS

This section validates the designed controller through simulation and comparative experiments. The simulation work is accomplished using MATLAB software. Specifically, corresponding models are constructed on the Simulink platform to verify the effectiveness of the proposed control strategy. During the Simulink simulation process, the simulation step size is set to 0.001 seconds.

The parameters for the quadcopter unmanned aerial vehicle system are as follows:  $g = 9.8m/s$   $J_r = 0.06kg \cdot m^2$   $J_z = 2.5 \times 10^{-2} kg \cdot m^2$   $K_z = K_\phi = K_\theta = K_\psi = 1.5 \times 10^{-2} kg \cdot m^2$   $J_x = J_y = 1.8 \times 10^{-2} kg \cdot m^2$   $m = 2.5kg$  The parameters for the

quadcopter unmanned aerial vehicle system are as follows:  $d_\Gamma = d_\Theta = [\sin(t), \sin(t), \sin(t)]^T$ , The initial state of the quadcopter drone is  $[1, -1, 1, 0, 0, 0, 1, -1, 1, 0, 0, 0]^T$ .

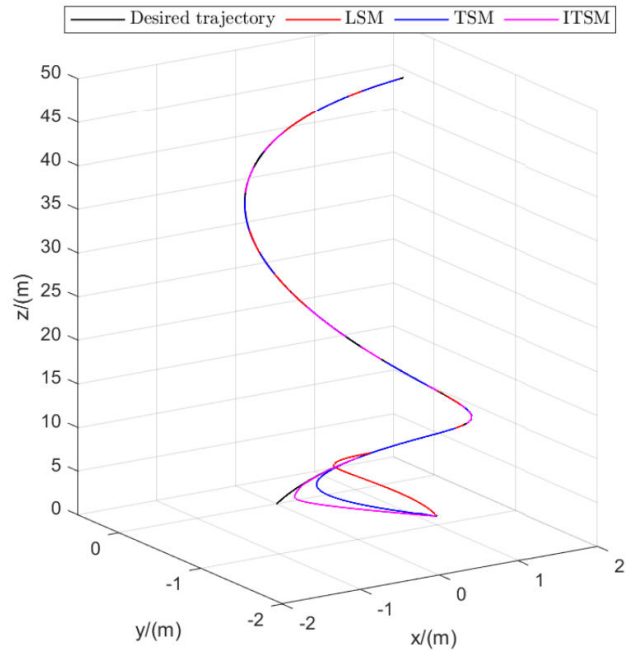
The parameter selection for the integral terminal sliding surface of the quadrotor is as follows: For the position subsystem:  $\lambda_{1\delta} = [90, 80, 70]^T$   $\lambda_{2\delta} = [20, 20, 20]^T$   $\gamma_{2\delta} = [0.8, 0.8, 0.8]^T$   $\gamma_{1\delta} = [0.95, 0.95, 0.92]^T$ , for the attitude subsystem:  $\lambda_{1\Theta} = [80, 80, 90]^T$   $\lambda_{2\Theta} = [30, 30, 10]^T$   $\gamma_{1\Theta} = [1, 1, 1, 1, 1]^T$   $\gamma_{2\Theta} = [4, 4, 1, 3]^T$

The parameter selection for the adaptive superhelix is as follows: for the position subsystem:  $\zeta_{1\delta} = [K_x, K_y, K_z]^T$   $\varepsilon_\delta = [12, 10, 12]^T$   $\vartheta_\delta = [0.4, 0.4, 0.4]^T$   $\mu_\delta = [0.04, 0.04, 0.04]^T$   $\zeta_{m\delta} = [1.8, 1.8, 1.8]^T$ ,  $\eta_\delta = [1.8, 1.8, 1.8]^T$   $\tau_\delta = [1, 1, 1]^T$

for the attitude subsystem:  $\zeta_{1\Theta} = [K_\phi, K_\theta, K_\psi]^T$   $\varepsilon_\Theta = [10, 10, 10]^T$   $\vartheta_\Theta = [0.4, 0.4, 0.4]^T$   $\mu_\Theta = [0.05, 0.05, 0.05]^T$   $\tau_\delta = [0.8, 0.8, 0.8]^T$   $\zeta_{m\Theta} = [0.2, 0.2, 0.2]^T$   $\eta_\Theta = [0.2, 0.2, 0.2]^T$

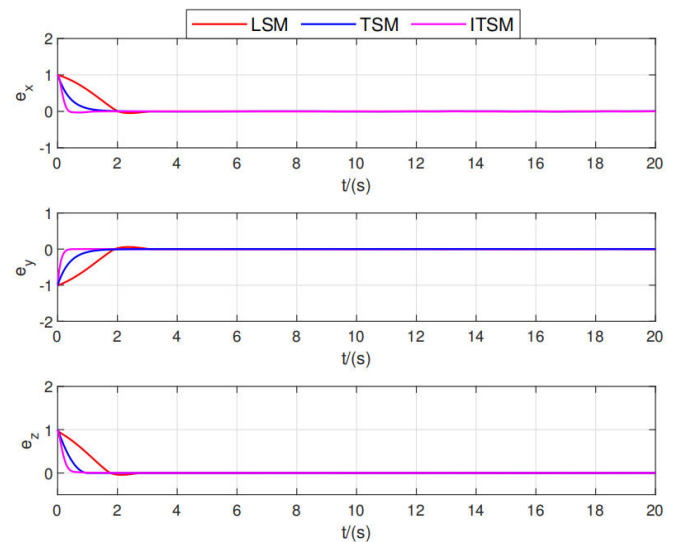
This chapter's comparative experiment employs the same adaptive superhelix control law, and the linear sliding surface is:  $S = \dot{e} + \rho e$ , where  $\rho = [40, 40, 40, 2, 2, 2]^T$ , the terminal sliding surface of the is  $S = \dot{e} + \beta e^\lambda$ , where  $\beta = [2, 10, 5, 10, 10, 5]^T$ ,  $\lambda = [0.5, 0.9, 0.9, 0.9, 0.9, 0.9]^T$ .

The trajectory tracking curves of the quadrotor unmanned aerial vehicle in the three-dimensional space are shown in Figure (a). From this curve, it can be clearly observed that, compared with the linear sliding mode control strategy and the terminal sliding mode strategy, the control strategy proposed in this section demonstrates significant advantages in terms of convergence speed and tracking accuracy.

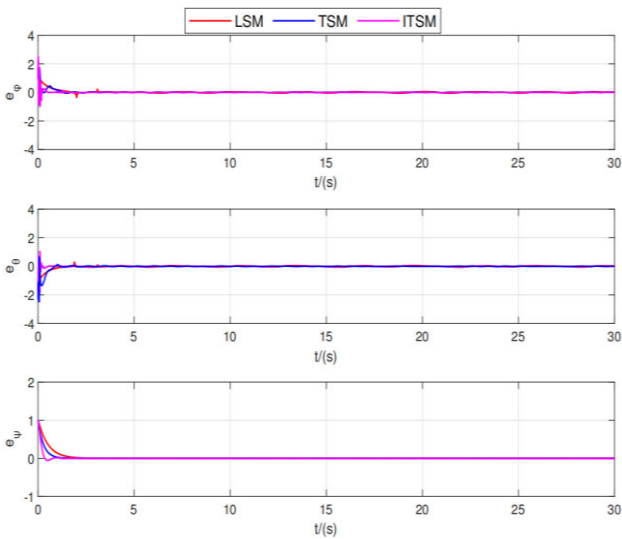


(a) 3-D spiral trajectory

Figures (b) and (c) present the tracking errors of the position subsystem and the attitude subsystem of the quadrotor unmanned aerial vehicle. It can be observed that the convergence speed of the direction in this paper's method is significantly better than that of LSM and TSM. The position subsystem of the control strategy proposed in this paper converges to zero with an error around 0.6 seconds, while the linear sliding mode position subsystem converges in about 1.98 seconds and the terminal sliding mode converges in about 1.2 seconds. From Figure (c), it can be seen that the controller designed in this paper has a faster and smoother attitude tracking error convergence, with higher error accuracy.

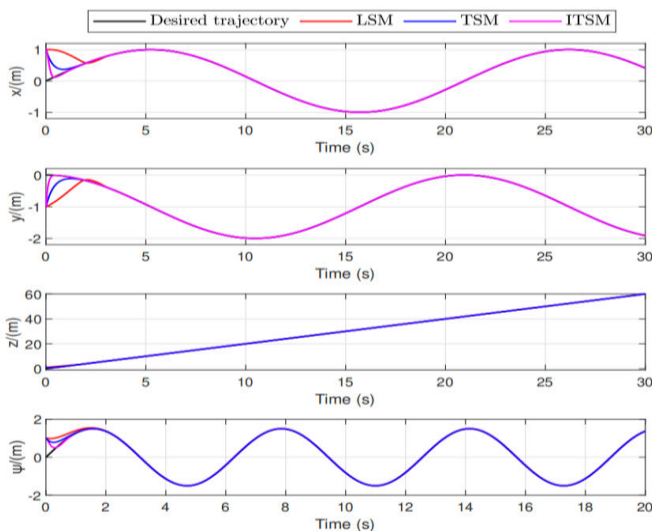


(b) Position subsystem trajectory tracking error



(c) Attitude subsystem trajectory tracking error

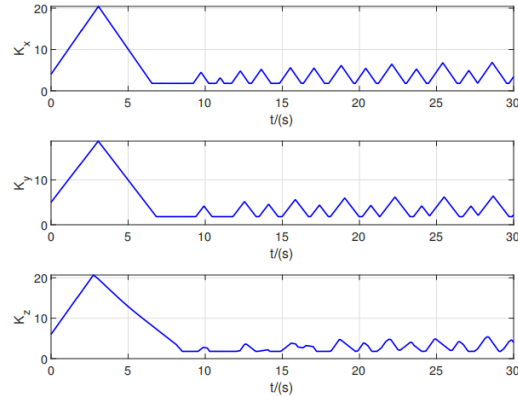
Figure (d) shows the tracking curves of the heading  $x$ ,  $y$ ,  $z$  and yaw angle  $\psi$  based on the adaptive hyper-spiral sliding mode control. It can be seen that each control strategy can track the desired trajectory. However, the control strategy designed in this paper has a better tracking effect. In the heading  $x$ ,  $y$  and yaw  $\psi$  directions, it significantly outperforms the other two sliding mode control strategies in terms of faster tracking to the desired trajectory.



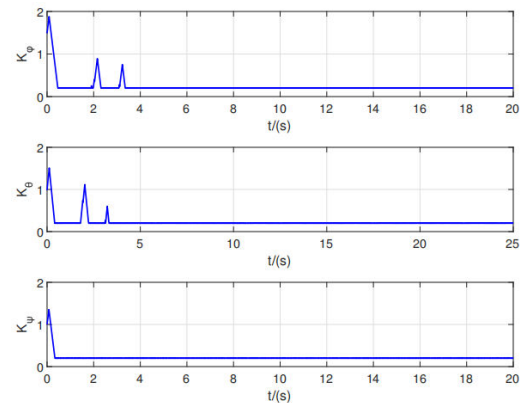
(d) Position and posture tracking curves

Figures (e) and (f) show the adaptive gain diagram based on the adaptive hyper-spiral integral terminal sliding mode

control. For the position subsystem, the disturbance is smaller within the range of 5s to 10s, and the gain is lower. After 10s, the gain increases as the disturbance increases and decreases as the disturbance decreases, avoiding the adverse effects of high gain and ensuring the convergence of the sliding surface. This verifies the effectiveness of the adaptive law.



(e) Position subsystem adaptive law



(f) Posture subsystem adaptive law

### V. CONCLUSION

In the process of position and attitude trajectory tracking control for quadrotor unmanned aerial vehicles, uncertainties and external disturbances are encountered, and the sliding mode control may suffer from chattering phenomena in practical applications. This paper combines two chattering suppression methods: gain adaptation and super-spiral sliding mode control, and proposes a position and attitude control method for quadrotor aircraft with time-varying disturbances, the Adaptive Super-Spiral Integral Terminal Sliding Mode Control (ASTISMC) algorithm. In this case, the dynamic gain ensures robustness to disturbances, reduces the amplitude of the controller, and effectively suppresses chattering. Moreover, it does not require prior knowledge of the disturbance bounds. By combining nonsingular terminal sliding mode and integral sliding mode, the singularity problem existing in traditional terminal sliding mode control is solved. By introducing nonlinear terms and integral terms, the nonsingular integral terminal sliding mode control can effectively reduce the chattering phenomenon of the system and improve the smoothness of the control signal. The stability of the closed-loop system is analyzed using the Lyapunov function. Finally, the effectiveness and success of

this method are verified through simulation and experiments, and it is compared with other tracking methods in terms of tracking performance and robustness. ASTISMC has smaller steady-state error, faster response speed, and performs better in reducing the chattering phenomenon during the control process.

flight evaluations[J]. IEEE Transactions on control systems technology, 2013, 21(4): 1400-1406.

#### REFERENCES

- [1] K. Xia, X. Li, X. Li, et al. Cooperative Tracking of Quadrotor UAVs Using Parallel Optimal Learning Control[J]. IEEE Trans. Autom. Sci. Eng, 2024.
- [2] G. Sun, X. Zhang, Y. Liu, et al. Safety-Driven and Localization Uncertainty-Driven Perception-Aware Trajectory Planning for Quadrotor Unmanned Aerial Vehicles[J]. IEEE Trans. Intell. Transp. Syst, 2024.
- [3] H. Huang, A.V. Savkin and W. Ni. Online UAV trajectory planning for covert video surveillance of mobile targets[J]. IEEE Trans. Autom. Sci. Eng, 2021, 19(2):735-746.
- [4] X. Zhou, X. Yu, K.Guo, et al. Safety flight control design of a quadrotor UAV with capability analysis[J]. IEEE Trans. Cybern, 2021, 53(3): 1738-1751.
- [5] M. Zare, F. Pazooki and S.E Haghghi. Quadrotor UAV position and altitude tracking using an optimized fuzzy-sliding mode control[J]. IETE J. Res, 2022, 68(6):4406-4420.
- [6] O.A. Jasim and S.M. Veres. A robust controller for multi rotor UAVs[J]. Aerosp. Sci. Technol, 2020, 105:106010.
- [7] Romero, S. Sun, P. Foehn, et al. Model predictive contouring control for time-optimal quadrotor flight[J]. IEEE Trans. Rob, 2022, 38(6): 3340-3356.
- [8] Q. Han, Z. Liu, H. Su, et al. Filter-based disturbance observer and adaptive control for Euler-Lagrange systems with application to a quadrotor UAV[J]. IEEE Trans. Ind. Electron, 2022, 70(8): 8437-8445.
- [9] P.K. Muthusamy, M. Garratt, H. Pota, et al. Real-time adaptive intelligent control system for quadcopter unmanned aerial vehicles with payload uncertainties[J]. IEEE Trans. Ind. Electron, 2021, 69(2): 1641-1653.
- [10] X. Shao, G. Sun, W. Yao, et al. Adaptive sliding mode control for quadrotor UAVs with input saturation[J]. IEEE/ASME Trans. Mechatron, 2021, 27(3): 1498-1509.
- [ ] Zheng E H, Xiong J J, Luo J L. Second order sliding mode control for a quadrotor UAV[J]. ISA Trans, 2014, 53(4): 1350-1356.
- [ ] Razmi H, Afshinfar S. Neural network-based adaptive sliding mode control design for position and attitude control of a quadrotor UAV[J]. Aerosp. Sci. Technol, 2019, 91: 12-27.
- [ ] Yu X, Zhihong M. Fast terminal sliding-mode control design for nonlinear dynamical systems[J]. IEEE Trans. Circuits Syst. I Regul. Pap, 2002, 49(2): 261-264.
- [ ] Feng Y, Yu X H, Man Z H. Non-singular terminal sliding mode control of rigid manipulators [J]. Automatica, 2002, 38 (12): 2159–2167.
- [ ] Yang L, Yang J Y. Nonsingular fast terminal sliding-mode control for nonlinear dynamical systems [J]. International Journal of Robust and Nonlinear Control, 2011, 21 (16): 1865–1879.
- [ ] Chiu C S. Derivative and integral terminal sliding mode control for a class of MIMO nonlinear systems [J]. Automatica, 2012, 48 (2): 316–326.
- [ ] Mofid O, Mobayen S, Zhang C, et al. Desired tracking of delayed quadrotor UAV under model uncertainty and wind disturbance using adaptive super-twisting terminal sliding mode control[J]. ISA Trans, 2022, 123: 455-471.
- [ ] Dydek Z T, Annaswamy A M, Lavretsky E. Adaptive control of quadrotor UAVs: A design trade study with